RSC Advances

PAPER

View Article Online
View Journal | View Issue

Check for updates

Cite this: *RSC Adv.*, 2020, **10**, 13968

# Understanding $CO_2$ capture kinetics and energetics by ionic liquids with molecular dynamics simulation

Fan Yang,†[a] Xianjuan Wang,†[a] Yang Liu,[a] Yanmei Yang,[b] Mingwen Zhao,[a] Xiangdong Liu*[a] and Weifeng Li*[a]

Room temperature ionic liquids (ILs) are recognized to be potential media for $CO_2$ capture, but the interaction nature is less documented which hinders the future development of ILs with high $CO_2$ solvation capability. Here, through all atom molecular dynamics (MD) simulations, the solvation process of $CO_2$ with four representative ILs, [EMIM][$BF_4$], [BMIM][$BF_4$], [EMIM]CL and [BMIM]CL was systematically studied. Our data clearly reflect the fact that hydrophobic components from both cations and anions dominate $CO_2$ solvation because IL–$CO_2$ attraction is mainly driven by the van der Waals attractions. Consequently, cations with longer alkyl chain (for instance, $[BMIM]^+$ than $[EMIM]^+$) and anions with higher hydrophobicity (for instance, $[BF_4]^-$ than $CL^-$) effectively enhance $CO_2$ solvation. For all the ILs under study, addition of water into ILs abates $CO_2$ solvation through regulating the anion–$CO_2$ interactions. Moreover, it is worth mentioning that ILs with a hydrophobic anion ($[BF_4]^-$ in this study) are more resistant to the existence of water to capture $CO_2$ than ILs with a hydrophilic anion ($Cl^-$ in this study). Free energy decomposition analyses were conducted which support the above findings consistently. Generally, it is predicted that cations with long alkyl chain, anions with high hydrophobicity, and ILs with smaller surface tension are potentially effective $CO_2$ capturing media. Our present study helps the deep understanding of the $CO_2$ capturing mechanism by ILs and is expected to facilitate the future design and fabrication of a novel IL medium for gas capture and storage.

Received 13th December 2019
Accepted 16th March 2020

DOI: 10.1039/d0ra02221g

rsc.li/rsc-advances

Open Access Article. Published on 06 April 2020. Downloaded on 1/23/2026 4:05:47 PM.
This article is licensed under a Creative Commons Attribution-NonCommercial 3.0 Unported Licence.

## 1. Introduction

Room temperature ionic liquids (ILs) are a new class of organic salts whose melting temperature falls below the conventional limit of 100 °C. Compared with conventional organic solvents, they possess many intriguing qualities, such as low vapor pressure, low toxicity, and high thermodynamic stability which have made these ionic compounds the solvents of choice for the so-called green chemistry.[1,2]

ILs are regarded as potential candidates for $CO_2$ storage, the dominant reason for the global warming process.[3] It is remarkable that, compared with the conventional amine scrubbing approach,[4] the organic and non-volatilizing nature of ILs can effectively decrease the energy cost for $CO_2$ capture and avoid the concern of causing environmental pollution.[5] For instance, Liu *et al.* have reported single-stage and multi-stage $CO_2$ adsorption processes by ILs which could effectively decrease the electrical and thermal energy costs by 42.8% and 66.04%, respectively.[6] Moreover, several ILs demonstrated $CO_2$-selective capturing capability which can be utilized for the purpose of $CO_2$ separation and purification from gas mixture.[7] Numerous research groups have systematically studied the capturing capacity of various ILs for various gases, including $CO_2$, $CH_4$, $H_2$ and so on, by both experimental and theoretical approaches.[1,2,8–15] Ramdin *et al.* experimentally studied the $CO_2$ solubility and diffusivity in numbers of ILs and proposed that ILs have great solubility capacity to $CO_2$.[1] Anthony *et al.* reported that 1-*n*-butyl-3-methlimidazolium hexafluorophosphates have strong dissolving ability for $CO_2$.[2] Bates *et al.* discovered that a new room temperature ionic liquid (TSIL) has a considerable capacity to capture $CO_2$ effectively, compared to the commercial amine sequestering reagents.[13] Kerle *et al.* further reported that $CO_2$ solubility is dependent to the alkane chain length of ILs.[12] Shi *et al.* discovered that the ionic liquid ([HMIM][$Tf_2N$]) demonstrates strong interaction with $CO_2$, by conducting Monte Carlo simulations, which is six times stronger than the interaction between ILs and $H_2$.[15]

Albeit a large number of works that have been conducted experimentally, the effective $CO_2$ capture and storage are still challenges. Previous experiments have evaluated the effects of introduction of water to ILs for $CO_2$ capture. For instance, Bermejo *et al.* have systematically explored the effects of water in ILs

[a]*School of Physics and State Key Laboratory of Crystal Materials, Shandong University, Jinan, Shandong, 250100, China. E-mail: xdliu@sdu.edu.cn; lwf@sdu.edu.cn*

[b]*College of Chemistry, Chemical Engineering and Materials Science, Collaborative Innovation Center of Functionalized Probes for Chemical Imaging in Universities of Shandong, Key Laboratory of Molecular and Nano Probes, Ministry of Education, Institute of Molecular and Nano Science, Shandong Normal University, Jinan, 250014, China*

† These authors contribute equally to this work.



This journal is © The Royal Society of Chemistry 2020

Open Access Article. Published on 06 April 2020. Downloaded on 1/23/2026 4:05:47 PM.
This article is licensed under a Creative Commons Attribution-NonCommercial 3.0 Unported Licence.

on $CO_2$ solubility and found that only small ratio of water in ILs is favorable to $CO_2$ solvation. In contrast, high concentration of water reversely lowered the $CO_2$ solubility.[16] Unfortunately, the molecular mechanism of the influence of water on the performance of ILs is still unknown. This situation becomes to be the main obstacle to the design and development of high-performance ILs for the aim of effective $CO_2$ capture and storage.

In this work, the solvation process of $CO_2$ by several ILs is studied by atomic molecular dynamics (MD) simulations. Four experimentally widely-studied ILs and the corresponding hydrated states were adopted as the representative solvents. Several key characters of ILs, including the specific types of cations and anions, the length of the alkyl chain, *etc.*, have been systemically assessed on $CO_2$ solvation. We sincerely hope that our present study could help the better and deep understanding of $CO_2$ capturing mechanism by ILs and facilitate the future design and fabrication of novel IL medium for gas capture and storage.

## 2. Model setup and simulation details

All the MD simulations were performed with the GROMACS 5.1.3 package[17] with GPU acceleration. Four types of representative ILs which are commonly studied in the experiments have been considered: [BMIM][$BF_4$], [EMIM][$BF_4$], [BMIM]CL and [EMIM]CL. The force field parameters developed by Chaban *et al.* through quantum mechanics calculations were used for ILs.[18] TIP3P water model[19] and the EMP2 $CO_2$ model[20] were used. During the simulation, a leap-frog algorithm was used to integrate Newton's equations of motion, and the time step was set to 2 fs. All the covalent bonds were constrained by the LINCS algorithm.[21] The cut-off for the short-range electrostatics and Lennard–Jones interactions were both set to 1.0 nm and the particle mesh Ewald (PME) algorithm[22] was used to deal with the long-range electrostatic interactions. The simulation systems were firstly optimized by an energy minimization with the steepest descent algorithm to generate an appropriate starting configuration, and then equilibrated for 500 ps at NPT ensemble to reach the reference temperature of 300 K and the reference pressure of 1 bar, respectively. Then 100 ns trajectory was generated for data collection at the NVT ensemble.

In addition to the normal MD simulations, we further studied the $CO_2$ solvation energetics in ILs by calculating the solvation free energy ($\Delta G$) using the Free Energy Perturbation (FEP) method.[23,24] To study the effects of water contents in the ILs, we have considered a series of water molar concentrations in the range of 0–96.2%. The components in the simulation boxes were depicted in Fig. 1. In the FEP calculations, 21 values were used for the coupling parameter $\lambda$ with a resolution of 0.05. The process was divided into two parts: the perturbation of electrostatic interaction and the perturbation of van der Waals (vdW) interaction.

## 3. Results and discussion

### 3.1 $CO_2$ solvation in pure water and ILs

As the main aim of the current work is to understand the $CO_2$ storage capability of ILs through a mechanism view of the solvation free energetics, the benchmark study of the $CO_2$ solvation free energy in pure water (abbreviated as $\Delta G_{water}$) is desired. The current molecular models gave a theoretical prediction of $\Delta G_{water} = 1.80$ kJ mol$^{-1}$ at 300 K. Compared to previous studies (Table 1), this agrees well with the experimental value of 1.005 kJ mol$^{-1}$.[25] To verify the validity of our present models of $CO_2$ and ILs, we have calculated the solvation free energy of $CO_2$ in pure [BMIM][$BF_4$] at the 323 K and obtained a value of $-1.00$ kJ mol$^{-1}$. This is well consistent with experimental value of $-1.005$ kJ mol$^{-1}$ reported by Cadena *et al.*[26]

In the following, we explore the solvation characteristics of $CO_2$ in pure ILs at room temperature (300 K). Using the same setups in the above calculations, the solvation free energy of $CO_2$ in ILs (abbreviated as $\Delta G_{IL}$) are calculated which are: $-1.69$ kJ mol$^{-1}$ in [EMIM][$BF_4$], $-2.09$ kJ mol$^{-1}$ in [BMIM][$BF_4$], $-0.87$ kJ mol$^{-1}$ in [EMIM]CL and $-1.92$ kJ mol$^{-1}$ in [BMIM]CL, respectively. Compared with the value in pure water of 1.80 kJ mol$^{-1}$, the negative values clearly indicate that $CO_2$ molecule is better dissolved in ILs which is consistent with experimental reports.

Deduced from four $\Delta G_{IL}$, the trend of $CO_2$ dissolving capacities of the four ILs is as follows: [BMIM][$BF_4$] > [BMIM][CL] > [EMIM][$BF_4$] > [EMIM][CL]. Amongst them, the [BMIM][$BF_4$] has the highest dissolving capacity for $CO_2$. When comparing the cations, it is found that the length of the alkyl chain of cations has a positive correlation to $CO_2$ solubility when the anion is same: [BMIM][$BF_4$] > [EMIM][$BF_4$]. In detail, the $\Delta G_{IL}$ in [BMIM][$BF_4$] is $-0.40$ kJ mol$^{-1}$ lower than that of [EMIM][$BF_4$]. These results are consistent with the experimental reports by Camper[29] and Anthony.[30] For two Chloride ILs, the trend is same: [BMIM][CL] > [EMIM][CL]. The free energy difference is even larger, which is $-1.05$ kJ mol$^{-1}$. This is well consistent with previous experimental observations by Yunus[31] and Aki.[32] In addition, the specific types of anions also play a minor role. The $\Delta G_{IL}$ of two $[EMIM]^+$ ILs differs by $-0.82$ kJ mol$^{-1}$ when a $[BF_4]^-$ is replaced by $Cl^-$. While for the two $[BMIM]^+$ ILs, the difference is smaller which is $-0.17$ kJ mol$^{-1}$. This is mainly attributed to the effective volumes (in other words, the hydrophobicity) of the anions which will be presented below in detail. It is worth mention that Zhang *et al.* also have demonstrated that the increase in alkyl chain of cation and the fluoration of anions or cations are beneficial to capture $CO_2$.[33,34]

In order to probe the dominating molecular components that play the key role in the solvation process of $CO_2$ in pure ILs, we analyzed the radial distribution functions (RDFs) of the imidazole ring, alkyl chain and anion around the center of mass (COM) of the $CO_2$ molecule. As depicted in Fig. 2a and b, the first interaction shell (beginning from 0.25–0.3 nm) around $CO_2$ is uniformly from the anions for both $[BF_4]^-$ and $Cl^-$. For comparison, the RDF peaks representing cation begin at a larger distance, ~0.42 nm from $CO_2$. These results indicate the fact that anions form direction interactions with $CO_2$. Especially that for the $[BF_4]^-$, it forms more intimate interactions, through the Fluorine atoms, with $CO_2$ with a closer distance of ~0.25 nm. The compact anion shell, to certain

Open Access Article. Published on 06 April 2020. Downloaded on 1/23/2026 4:05:47 PM.
This article is licensed under a Creative Commons Attribution-NonCommercial 3.0 Unported Licence.

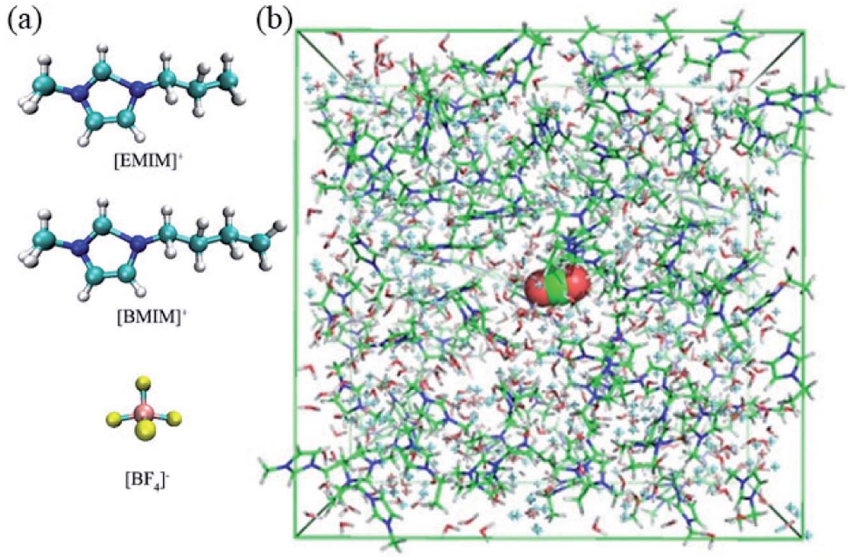


Fig. 1 (a) Molecular structures of $[BMIM]^+$, $[EMIM]^+$ and $[BF_4]^-$; (b) snapshot of the simulated box. The $CO_2$ molecule is placed at the box center.

Table 1 The $CO_2$ solvation free energy in pure water from current study and previous literatures

| Method | $\Delta G_{water}$ | Ref. |
|---|---|---|
| MD | 1.80 | This work |
| QM/MM | 0.042 | 27 |
| MM | 9.54 | 27 |
| Quasi chemical theory | 0.25 | 28 |
| Experiment | 1.005 | 25 |

extent, prevents cations from interacting with $CO_2$. These phenomena are consistent with experimental results by Anthony[30] and Zhang.[35] As monovalent anions, the $[BF_4]^-$ clearly has a larger volume than $Cl^-$. Thus, $[BF_4]^-$ is relatively more hydrophobic than $Cl^-$. Zhang *et al.* also reported that [HMIM][FEP] has higher $CO_2$ solubility than [HMIM][$TF_2N$] experimentally because of the longer fluoroalkyl chain of [FEP].[35]

Further, we qualitatively compared different parts of cations in contacting with $CO_2$. For brief, the imidazole ring of the cation is named as 'head' and the alkyl chain is named as 'tail' as depicted in the insert of Fig. 2a. For the four ILs, the heights of RDF peaks representing $CO_2$–tail interactions are always higher than that of $CO_2$–head interactions at the similar distance, regardless of the specific types of anions. Especially for the chloride ILs (Fig. 2b), there is almost no apparent peaks for the $CO_2$–head interactions. This points to the fact that the alkyl chains of cations play the more important role in $CO_2$ solvation and, more precisely, longer alkyl chain results in lower $\Delta G_{IL}$.

In combination with above anion analyses, it can be concluded that $CO_2$ prefers to interact with hydrophobic components of cation and hydrophobic anions, although $CO_2$

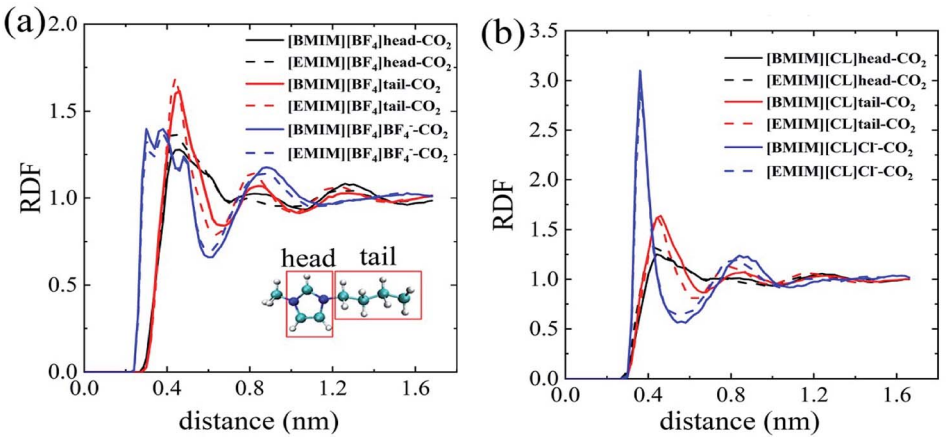


Fig. 2 The radial distribution functions of ILs atoms around $CO_2$ center of mass (COM). (a) $[BMIM][BF_4]$ solid line; $[EMIM][BF_4]$ dotted line; (b) [BMIM][CL] solid line; [EMIM][CL] dotted line.

 This journal is © The Royal Society of Chemistry 2020

Open Access Article. Published on 06 April 2020. Downloaded on 1/23/2026 4:05:47 PM.
This article is licensed under a Creative Commons Attribution-NonCommercial 3.0 Unported Licence.

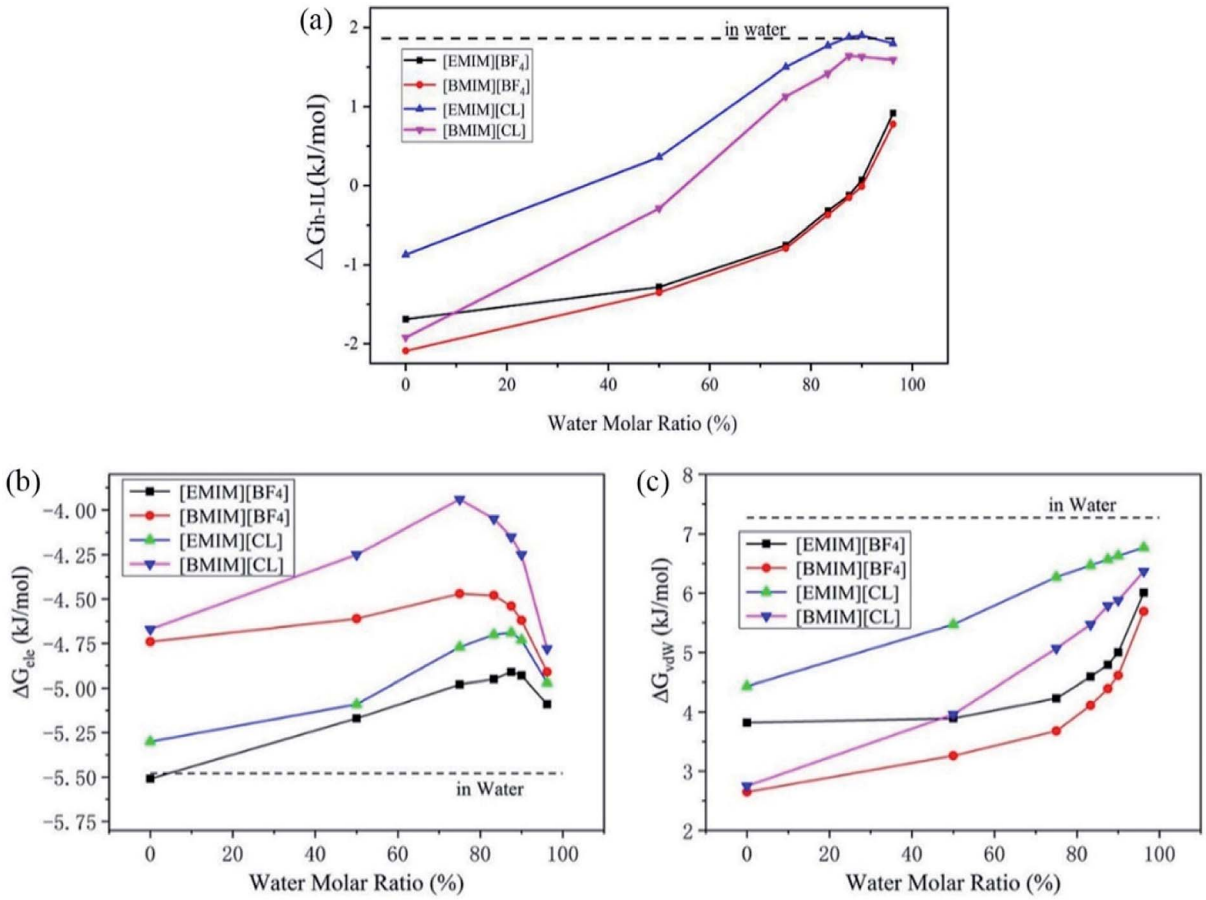


Fig. 3 The change tendency of (a) total $CO_2$ solvation free energy, (b) electronic component and (c) van der Waals component in hydrated ILs with different water molar ratio. The dashed lines represent the corresponding values in pure water.

carries a dipole. Thus, it is a feasible way to search the suitable ILs with long alkyl chains or fluorinate anions for $CO_2$ capture.

### 3.2 The effect of water in ILs on $CO_2$ solvation

Previous experiments have demonstrated that the existence of water highly regulates $CO_2$ capture. In detail, Bermejo *et al.* reported that small ratio of water in ILs is favorable to $CO_2$ dissolving. In contrast, high concentration of water will reversely lower the $CO_2$ solubility.[16] Goodrich *et al.* also reported that the presence of water in ILs effectively reduced the $CO_2$ storage capacity.[36] Wang *et al.* reported that compared to pure triethylbutylammonium acetate ([$N_{2224}$][Ac]), the introduction of $H_2O$ in [$N_{2224}$][Ac] reduced the $CO_2$ adsorption.[37] However, the underline physical mechanism that accounts for the lowered performance of ILs is still poorly documented. To explain these experimental observations, we have considered the solvation of $CO_2$ in a serious of hydrated ILs with molar ratios of water increased from 0% (pure ILs) to 96.2% (diluted ILs) and calculated the $CO_2$ solvation free energies, $\Delta G_{\text{h-IL}}$.

From Fig. 3a, it is very interesting to find that the tendencies of change of $\Delta G_{\text{h-IL}}$ can be divided into two types according to anions. For Chloride ILs, the $\Delta G_{\text{h-IL}}$ increases more quickly with the introduction of water. At water concentration of 83.3%, they approach to the value of $\Delta G_{\text{water}}$ (1.80 kJ mol$^{-1}$). In contrast, $\Delta G_{\text{h-IL}}$ in [EMIM][$BF_4$] and [BMIM][$BF_4$] increases in a much lower manner and reaches to a plateau of 0.8–1.0 kJ mol$^{-1}$ when water content is as high as 96.2%.

Then, the total $\Delta G_{\text{h-IL}}$ is decomposed into the electrostatic ($\Delta G_{\text{ele}}$) and vdW ($\Delta G_{\text{vdW}}$) contributions which is essential for a deep understanding of the physical interactions between $CO_2$ and the solvents. As shown in Fig. 3b, the $\Delta G_{\text{ele}}$ term is always negative which reveals that energy–favorable interactions such as charge–charge and dipole–dipole attractions between $CO_2$ and pure/hydrated ILs is the driving force for $CO_2$ capture. In hydrated ILs, the $\Delta G_{\text{ele}}$ term firstly increases (weakened electrostatic interactions) at low water contents and the profiles reach to the maximum at a water content of ~75% for two $[BMIM]^+$ ILs, and ~87.5% for two $[EMIM]^+$ ILs. After that, further increasing water content reversely decreases the $\Delta G_{\text{ele}}$ (re-strengthened electrostatic interactions) which favors $CO_2$ capture. This interesting transition is attributed to the formation of intimate interactions of $CO_2$ with excess water molecules (more discussions are presented below from RDF analyses). It is worth mention that, the water fractions in ILs are relatively small in the experiments (which is typically lower than 30%). Thus, the current results support the previous observations

Open Access Article. Published on 06 April 2020. Downloaded on 1/23/2026 4:05:47 PM.
This article is licensed under a Creative Commons Attribution-NonCommercial 3.0 Unported Licence.

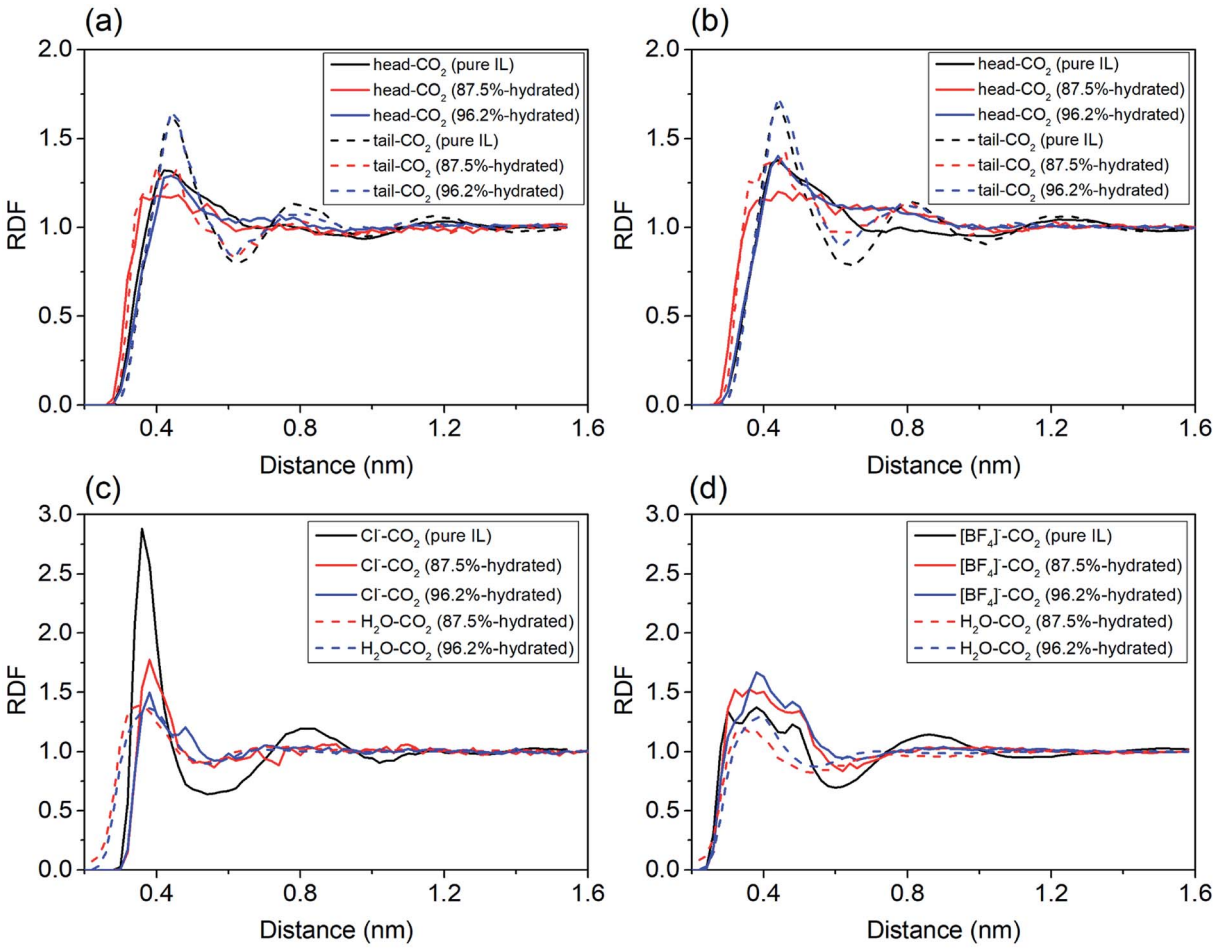


Fig. 4 The radial distribution functions of solution components around $CO_2$ in pure, 87.5% and 96.2% hydrated ILs. (a) and (c): [EMIM][CL]; (b)and (d) [EMIM][$BF_4$].

because the experimental conditions correspond to the weakened $\Delta G_{ele}$ range in Fig. 3b.

For the van der Waals interactions, it represents the energy consumption for introducing a cavity inside the solution thus the $\Delta G_{vdW}$ is positive. As shown in Fig. 3c, the $\Delta G_{vdW}$ is monotonically increasing with the addition of water. Considering the nature of van der Waals interactions, this reflects that the surface tension of the hydrated ILs increases because more energy is required to introduce the cavity for $CO_2$ molecule inside it. The $\Delta G_{vdW}$ increase is considerably larger than $\Delta G_{ele}$ decrease. Thus, the overall solubility of $CO_2$ in ILs generally decreases with addition of water. Moreover, as depicted in Fig. 3a, the $CO_2$ solubility in ILs with $[BF_4]^-$ anion is less regulated by water. From the decomposition analyses, this is

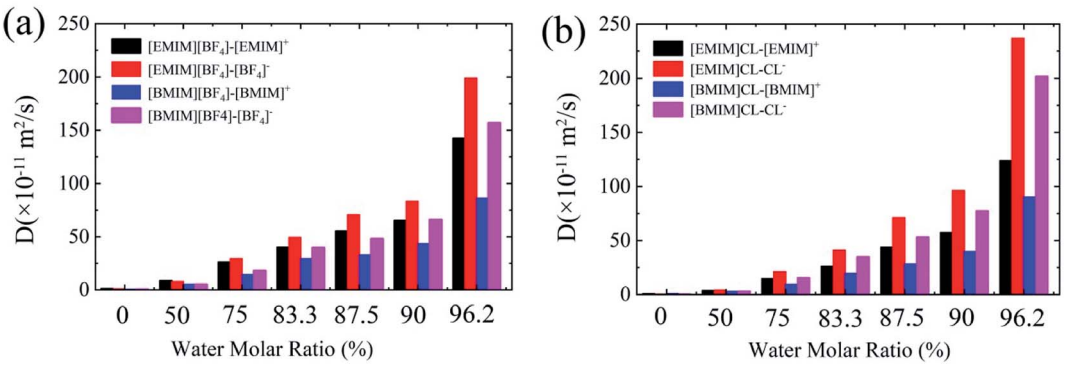


Fig. 5 The diffusion coefficients of cations and anions in pure and hydrated ILs.

 This journal is © The Royal Society of Chemistry 2020

Open Access Article. Published on 06 April 2020. Downloaded on 1/23/2026 4:05:47 PM.
This article is licensed under a Creative Commons Attribution-NonCommercial 3.0 Unported Licence.

mainly caused by the slower increase of $\Delta G_{vdW}$ term in two $[BF_4]^-$ ILs than that in $Cl^-$ ILs. Thus it can be seen that smaller surface tension and stronger electrostatic interaction with $CO_2$ are two favorable factors to improve the $CO_2$ solubility in ILs.

To probe the role of water in preventing ILs from adsorbing $CO_2$, we analyzed spatial distributions of water, imidazole ring (head), alkyl chain (tail) and anions around the COM of $CO_2$. For cations in IL with water ratio from 0–87.5%, the first peaks representing both head–$CO_2$ and tail–$CO_2$ bindings uniformly decreased in [EMIM][CL] (Fig. 4a) and [EMIM][$BF_4$] (Fig. 4b). This reflects a fact that the cation–$CO_2$ interactions were suppressed, resulting in $\Delta G_{ele}$ increase during this range which adopted the maximum value at water ratio of 87.5% as shown in Fig. 3b. Then, when further increasing water ratio from 87.5% to 96.2%, an interesting reverse trend was observed: these peaks reversely increased and were almost comparable to that in pure ILs, revealing that the interactions of cation–$CO_2$ were almost recovered in diluted ILs. In addition to the formation of intimate binding of water to $CO_2$ (dashed lines in Fig. 4c and d), $\Delta G_{ele}$ was found to decrease at this range (Fig. 3b). For anions, it is also interesting to find that two anions demonstrated distinct different behaviors in response to water. For $Cl^-$ (Fig. 4c), the first binding shell of $Cl^-$–$CO_2$ dramatically decreases with addition of water. This is attributed to the strong hydrophilic nature of $Cl^-$ which favors to bind to water instead of $CO_2$. For $[BF_4]^-$ (Fig. 4d), the first binding shell increases, but in a slow manner, when water content increases, indicating that water always enhances the binding between $CO_2$ and $[BF_4]^-$. This is attributed to the large volume of $[BF_4]^-$ which is classified to be hydrophobic anion. Thus, the $\Delta G_{h\text{-}IL}$ of $CO_2$ in hydrated ILs with $Cl^-$ anion increases more dramatically than $[BF_4]^-$ as depicted in Fig. 3a.

By analyzing the RDFs, it is found that the dominate component to $CO_2$ solubility of hydrated ILs is from the anion because the influence of water is closely connected to the hydrophilicity of anions. The current theoretical results predict that ILs with hydrophobic anions are more robust to capture $CO_2$ when water exists.

### 3.3 Diffusions of ILs

One of the recognized features of ILs is the high viscosity that results in significantly lowered diffusion of the $CO_2$ adsorbates. Bermejo *et al.* reported that small ratio of water in ILs is favorable to $CO_2$ dissolving. In contrast, high concentration of water will reversely lower the $CO_2$ solubility.[16] While the introduction of water into ILs regulates the diffusion of $CO_2$, less is known about the relationship between IL's viscosity and $CO_2$ solubility. In the following, we examined the diffusion coefficients ($D$) of cation and anion, respectively, with respect to water contents using the Einstein relation.[38]

As summarized in Fig. 5, it is found that the values of $D$ of both anion and cation in hydrated ILs quickly increase with the increase of water content. For the four types of pure ILs under study, the $D$ is considerably low, with an order of $\sim 0.6 \times 10^{-11}$ $m^2\ s^{-1}$. In diluted ILs, the $D$ increases by around two orders. Moreover, comparing the four ILs, three aspects can be acquired: (1) the anions diffuse more quickly than cations, especially for Chloride ILs; (2) $[EMIM]^+$ diffuses quicker than $[BMIM]^+$ when anion is same; (3) $Cl^-$ diffuses quicker than $[BF_4]^-$ when cation is same. These phenomena are consistent to the Stokes–Einstein theory which predicts that molecules with smaller size can diffuse faster. Generally, from these data, $CO_2$ solvation in ILs is found to be negatively-correlated to the $D$ of hydrated ILs. More specifically, hydrated ILs benefits $CO_2$ diffusion, simultaneously it reduces $CO_2$ storage capability.

## 4. Conclusions

To summarize, by MD simulations, the key factors of ILs that determine $CO_2$ solvation were identified. For cations, the alkyl chain dominants $CO_2$ capture because longer alkyl chain could effectively enhance $CO_2$ solvation. While for anions, the hydrophobic species are proved to favor $CO_2$ solvation. From free energy decomposition analyses, this is attributed to the interacting character between $CO_2$ and the ILs which is mainly driven by the van der Waals attractions. The existence of water seriously abates $CO_2$ solvation energy for all the ILs which is attributed to the weakened anion–$CO_2$ interactions. More importantly, it is found that ILs with hydrophobic anions are more resistant to the existence of water to capture $CO_2$ than ILs with hydrophilic anions. Through our analyses, a conclusion was made that ILs with long alkyl chain, hydrophobic anions, smaller surface tension and stronger electrostatic interaction with $CO_2$ are indicative factors to improve the $CO_2$ solubility.

## Conflicts of interest

There are no conflicts to declare.

## Acknowledgements

This work is supported by the National Natural Science Foundation of China (Grant No. 11874238), the Basic Research Project of Natural Science Foundation of Shandong Province (Grant No. ZR2018MA034) and the Fundamental Research Funds of Shandong University.

## References

1 M. Ramdin, T. W. de Loos and T. J. Vlugt, *Ind. Eng. Chem. Res.*, 2012, **51**, 8149–8177.
2 J. L. Anthony, E. J. Maginn and J. F. Brennecke, *J. Phys. Chem. B*, 2002, **106**, 7315–7320.
3 S. Zeng, X. Zhang, L. Bai, X. Zhang, H. Wang, J. Wang, D. Bao, M. Li, X. Liu and S. Zhang, *Chem. Rev.*, 2017, **117**, 9625–9673.
4 H. Ahn, M. Luberti, Z. Liu and S. Brandani, *Int. J. Greenhouse Gas Control*, 2013, **16**, 29–40.
5 M. E. Boot-Handford, J. C. Abanades, E. J. Anthony, M. J. Blunt, S. Brandani, N. Mac Dowell, J. R. Fernández, M.-C. Ferrari, R. Gross and J. P. Hallett, *Energy Environ. Sci.*, 2014, **7**, 130–189.
6 X. Liu, Y. Huang, Y. Zhao, R. Gani, X. Zhang and S. Zhang, *Ind. Eng. Chem. Res.*, 2016, **55**, 5931–5944.

Open Access Article. Published on 06 April 2020. Downloaded on 1/23/2026 4:05:47 PM.
This article is licensed under a Creative Commons Attribution-NonCommercial 3.0 Unported Licence.

7 X. Zhang, X. Zhang, H. Dong, Z. Zhao, S. Zhang and Y. Huang, *Energy Environ. Sci.*, 2012, **5**, 6668.
8 S. Budhathoki, J. K. Shah and E. J. Maginn, *Ind. Eng. Chem. Res.*, 2015, **54**, 8821–8828.
9 A. Yokozeki and M. B. Shiflett, *Ind. Eng. Chem. Res.*, 2007, **46**, 1605–1610.
10 A. Yokozeki and M. B. Shiflett, *Appl. Energy*, 2007, **84**, 351–361.
11 D. Kerlé, R. Ludwig and D. Paschek, *Z. Phys. Chem.*, 2013, **227**, 167–176.
12 D. Kerlé, R. Ludwig, A. Geiger and D. Paschek, *J. Phys. Chem. B*, 2009, **113**, 12727–12735.
13 E. D. Bates, R. D. Mayton, I. Ntai and J. H. Davis, *J. Am. Chem. Soc.*, 2002, **124**, 926–927.
14 J. L. Anderson, J. K. Dixon and J. F. Brennecke, *Acc. Chem. Res.*, 2007, **40**, 1208–1216.
15 W. Shi, D. C. Sorescu, D. R. Luebke, M. J. Keller and S. Wickramanayake, *J. Phys. Chem. B*, 2010, **114**, 6531–6541.
16 M. D. Bermejo, M. Montero, E. Saez, L. J. Florusse, A. J. Kotlewska, M. J. Cocero, F. van Rantwijk and C. J. Peters, *J. Phys. Chem. B*, 2008, **112**, 13532–13541.
17 M. J. Abraham, T. Murtola, R. Schulz, S. Páll, J. C. Smith, B. Hess and E. Lindahl, *SoftwareX*, 2015, **1**, 19–25.
18 V. V. Chaban, I. V. Voroshylova and O. N. Kalugin, *Phys. Chem. Chem. Phys.*, 2011, **13**, 7910–7920.
19 M. F. Harrach and B. Drossel, *J. Chem. Phys.*, 2014, **140**, 174501.
20 H. Liu, S. Dai and D.-e. Jiang, *Nanoscale*, 2013, **5**, 9984–9987.
21 B. Hess, H. Bekker, H. J. Berendsen and J. G. Fraaije, *J. Comput. Chem.*, 1997, **18**, 1463–1472.
22 T. Darden, L. Perera, L. Li and L. Pedersen, *Structure*, 1999, **7**, R55–R60.
23 M. A. M. Latif, N. Micaêlo and M. B. A. Rahman, *Chem. Phys. Lett.*, 2014, **615**, 69–74.
24 K. Jumbri, N. M. Micaelo and M. B. Abdul Rahman, *Mol. Simul.*, 2017, **43**, 19–27.
25 J. Lide and H. P. R. Fredikse, *CRC Handbook of Chemistry and Physics*, CRC Press, 75th edn, 1995.
26 C. Cadena, J. L. Anthony, J. K. Shah, T. I. Morrow, J. F. Brennecke and E. J. Maginn, *J. Am. Chem. Soc.*, 2004, **126**, 5300–5308.
27 N. Prasetyo and T. S. Hofer, *J. Chem. Theory Comput.*, 2018, **14**, 6472–6483.
28 D. Jiao and S. B. Rempe, *J. Chem. Phys.*, 2011, **134**, 224506.
29 D. Camper, C. Becker, C. Koval and R. Noble, *Ind. Eng. Chem. Res.*, 2005, **44**, 1928–1933.
30 J. L. Anthony, J. L. Anderson, E. J. Maginn and J. F. Brennecke, *J. Phys. Chem. B*, 2005, **109**, 6366–6374.
31 N. M. Yunus, M. A. Mutalib, Z. Man, M. A. Bustam and T. Murugesan, *Chem. Eng. J.*, 2012, **189**, 94–100.
32 S. N. Aki, B. R. Mellein, E. M. Saurer and J. F. Brennecke, *J. Phys. Chem. B*, 2004, **108**, 20355–20365.
33 D. Almantariotis, T. Gefflaut, A. A. Padua, J.-Y. Coxam and M. Costa Gomes, *J. Phys. Chem. B*, 2010, **114**, 3608–3617.
34 X. Zhang, F. Huo, Z. Liu, W. Wang, W. Shi and E. J. Maginn, *J. Phys. Chem. B*, 2009, **113**, 7591–7598.
35 X. Zhang, Z. Liu and W. Wang, *AIChE J.*, 2008, **54**, 2717–2728.
36 B. F. Goodrich, J. C. de la Fuente, B. E. Gurkan, Z. K. Lopez, E. A. Price, Y. Huang and J. F. Brennecke, *J. Phys. Chem. B*, 2011, **115**, 9140–9150.
37 G. Wang, W. Hou, F. Xiao, J. Geng, Y. Wu and Z. Zhang, *J. Chem. Eng. Data*, 2011, **56**, 1125–1133.
38 Z. Tang, L. Lu, Z. Dai, W. Xie, L. Shi and X. Lu, *Langmuir*, 2017, **33**, 11658–11669.

 This journal is © The Royal Society of Chemistry 2020